Extended Abstracts of the 2014 International Conference on Solid State Devices and Materials, Tsukuba, 2014, pp794-795

Scanning Gate Imaging of Quantum Point Contacts and the Origin of the 0.7 Anomaly

Andrea Iagallo[1], Nicola Paradiso[1], Stefano Roddaro[1,2], Christian Reichl[3], Werner Wegscheider[3], Giorgio Biasiol[2], Lucia Sorba[1], Fabio Beltram[1], and Stefan Heun[1]

[1]NEST, Istituto Nanoscienze–CNR and Scuola Normale Superiore
Piazza San Silvestro 12, 56127 Pisa, Italy
Phone: +39-050-509119 E-mail: andrea.iagallo@sns.it
[2]Istituto Officina dei Materiali CNR, Laboratorio TASC, 34149 Trieste, Italy
[3]Solid State Physics Laboratory, ETH Zurich, Schafmattstrasse 16, 8093 Zurich, Switzerland

Abstract

The origin of the anomalous transport feature appearing in quasi-1D constrictions at conductance $G \approx 0.7 \times (2e^2/h)$ - the so-called 0.7 anomaly - represents a long standing puzzle. Several mechanisms were proposed to explain it, but a general consensus has not been achieved. A key open issue is the influence of point defects that can occur in these low-dimensional devices on this conductance anomaly. Here we adopt a Scanning Gate Microscopy (SGM) technique to map individual impurity positions in several quasi-1D constrictions and correlate these with conductance characteristics.

1. Introduction

The low-conductance regime of quasi-1D constrictions reveals an anomalous feature around $0.7 \times (2e^2/h)$ that breaks the quantization of the conductance in units of $G_0=2e^2/h$. The origin of this feature, known as the "0.7 anomaly", is much debated and was subject to intense investigation in the past [1-4]. In this work, we make use of the SGM technique to investigate the role of localized potential imperfections in driving the 0.7 anomaly. In an SGM measurement, a voltage-biased metallic tip of a cryogenic AFM is scanned at fixed distance over the surface of the device while its transport properties are being recorded. The SGM technique allows local control of the carrier density with ~nm resolution, and it can be used to directly determine whether impurities are present or not near a given constriction, and to know exactly their position.

In this work, we exploit the ability of SGM to perform gating [5-7] to carry out enhanced channel shifting measurements where a much larger area (few μm^2) is probed compared to traditional measurements. When the biased tip is scanned above the gates around the QPC centre, SGM measurements are indeed equivalent to performing a channel shifting experiment, in that the constriction opening is moved laterally. Besides this ability, SGM proved to be extremely sensitive in probing the potential landscape of two-dimensional electron systems [8-10]. This high sensitivity in detecting conductance variations makes the SGM technique an ideal tool to investigate the effect of potential imperfections on the conductance of constrictions. In the present work, we thus performed an SGM investigation in an area of several μm around the QPCs to detect the presence of charged impurities.

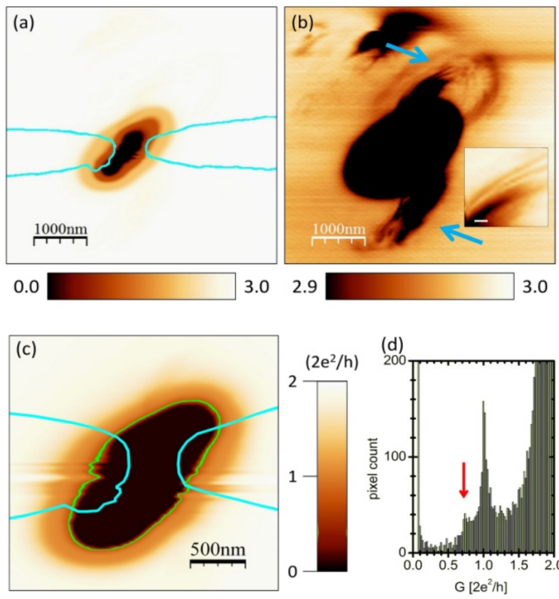

Fig. 1: Device A: QPC with localized impurities. (a) SGM scan of the differential conductance G of the QPC area, and (b) same data as in (a), after optimizing the contrast to highlight the presence of impurities (lower arrow) and of additional features caused by (anti)dot formation (upper arrow). G is in units of $G_0=2e^2/h$. (c) High resolution SGM image used to obtain the conductance histogram in (d), and displaying the annular symmetry retained by the 0.7 feature.

2. Experimental work

Our experiments were performed on 2DEGs obtained from single quantum well GaAs/AlGaAs heterostructures, where Hall bars with spli-gates were fabricated. Ohmic contacts (Ni/AuGe/Ni/Au) and Schottky electrodes (Ti/Au, 10 nm/20 nm) were deposited by thermal evaporation. Experiments were performed with over 10 devices fabricated from different heterostructures in a wide range of electron mobility μ ($2–12.5 \times 10^6$ cm^2/Vs) and density n ($1–5 \times 10^{11}$ cm^{-2}), all consistent with the conclusions presented here. As representative examples, in this work we present data from two devices A and B, whose mobility and density values were: $\mu_A=4.64 \times 10^6$ cm^2/Vs and $n_A=2.1 \times 10^{11}$ cm^{-2}, and $\mu_B=12.5 \times 10^6$ cm^2/Vs and $n_B=2.3 \times 10^{11}$ cm^{-2}. SGM measurements were performed by recording the source-drain conductance of the Hall bar as a function of tip position.

Figure 1(a) shows an SGM image of device A obtained by scanning the QPC area with a voltage V_{tip} = -2 V applied to the tip and V_g = -0.78 V to the gates. The image clearly displays the lowest three conductance plateaus, visible as annular concentric structures, and QPC pinch-off. By adjusting the contrast to enhance the visibility of small conductance variations, the impurities can be precisely identified, as shown in Fig. 1(b). In this device, the presence of the 0.7 anomaly is demonstrated by the peak in the conductance histogram in Fig. 1(d), which is further processed to give the spatial arrangement of the feature shown in Fig. 1(c): the 0.7 anomaly covers a closed annular structure around the QPC centre and runs parallel to the quantized conductance step. This result is not surprising for a clean constriction, where the 0.7 structure is expected to retain the same amplitude in all directions. However, in a device with point defects, both the amplitude and the shape of the 0.7 structure are expected to be substantially altered when the constriction is shifted near strong potential perturbations. These results show that a channel shifting measurement, even on a large scale as performed in this work, can be insufficient to detect the presence of impurities located at some ~100 nm from the QPC, and a large scale SGM probing of the potential is necessary instead.

Figure 2(a) shows an SGM image of the QPC area of device B, displaying the conductance range G = 0-$2e^2/h$. Beyond the standard SGM-induced electrostatic depletion of the constriction, we detect no trace of sharp potential fluctuations: differently from the case of sample A, we can rule out the presence of localized impurities in the scanned area.

We systematically checked an area of more than 5 µm radius around the QPC centre, and no localized scatterers were detected. The transport properties of device B and the conductance histogram, shown in fig. 2(c) and (d) respectively, confirm the presence of a marked 0.7 anomaly. The fact that we clearly observe the 0.7 anomaly in a constriction free of detectable defects, both in transport and in SGM measurements of the same device, allows us to discard any impurity-related mechanisms as the origin of the 0.7 anomaly.

3. Conclusions

In summary, we studied the occurrence of the 0.7 anomaly in QPCs with and without impurity-related localized potential fluctuations identified by SGM imaging. We observed the 0.7 structure with and without charged defects in proximity to the constriction and showed that it presents annular symmetry around the depleted spot at the QPC centre. These experiments show that any physical models based on localized defects (i.e. interference effects and Kondo effect due to localized quantum (anti)dots) for the 0.7 structure are not correct and that the latter is an intrinsic property of low-dimensional systems.

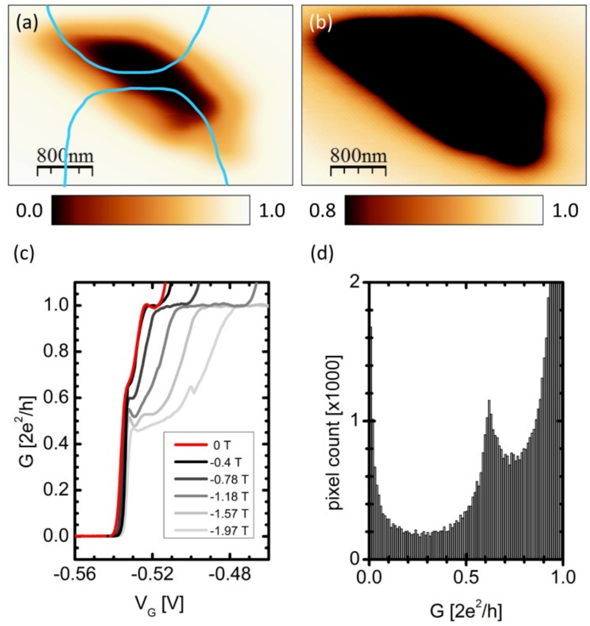

Fig. 2: Device B: QPC without localized impurities. (a) SGM image of the QPC area of device B. (b) High contrast version of image (a), showing a QPC constriction without any localized defect. G is given in units of $G_0=2e^2/h$. (c) Source-Drain conductance of device B as a function of gate voltage for different perpendicular magnetic fields. The evolution of the shoulder at $G \approx 0.65G_0$ to a value of $0.5G_0$, due to the removal of spin degeneracy, allows to identify the feature as the 0.7 anomaly. (d) Histogram of the SGM conductance map shown in (a).

References

[1] K. J. Thomas, J. T. Nicholls, M. Y. Simmons, M. Pepper, D. R. Mace, and D. A. Ritchie, Phys. Rev. Lett. **77**, 135 (1996).

[2] N. K. Patel, J. T. Nicholls, L. Martn-Moreno, M. Pepper, J. E. F. Frost, D. A. Ritchie, and G. A. C. Jones, Phys. Rev. B **44**, 13549 (1991).

[3] A. P. Micolich, J. Phys. Condens. Matter **23**, 443201 (2011).

[4] S. Xiang, S. Xiao, K. Fuji, K. Shibuya, T. Endo, N. Yumoto, T. Morimoto, N. Aoki, J. P. Bird and Y. Ochiai, J. Phys.: Condens. Matter **26**, 125304 (2014).

[5] M. A. Topinka, B. J. LeRoy, S. E. J. Shaw, E. J. Heller, R. M. Westervelt, K. D. Maranowski, and A. C. Gossard, Science **289**, 2323 (2000).

[6] B. J. LeRoy, A. C. Bleszynski, K. E. Aidala, R. M. Westervelt, A. Kalben, E. J. Heller, S. E. J. Shaw, K. D. Maranowski, and A. C. Gossard, Phys. Rev. Lett. **94**, 126801 (2005).

[7] N. Paradiso, S. Heun, S. Roddaro, L. Sorba, F. Beltram, G. Biasiol, L. N. Pfeiffer, and K. W. West, Phys. Rev. Lett. **108**, 246801 (2012).

[8] M. A. Topinka, B. J. LeRoy, R. M. Westervelt, S. E. J. Shaw, R. Fleischmann, E. J. Heller, K. D. Maranowski, and A. C. Gossard, Nature **410**, 183 (2001).

[9] M. P. Jura, M. A. Topinka, L. Urban, A. Yazdani, H. Shtrikman, L. N. Pfeiffer, K. W. West, and D. Goldhaber-Gordon, Nat. Phys. **3**, 841 (2007).

[10] N. Paradiso, S. Heun, S. Roddaro, G. Biasiol, L. Sorba, D. Venturelli, F. Taddei, V. Giovannetti, and F. Beltram, Phys. Rev. B **86**, 085326 (2012).